반도체 소자 측정 및 분석기법

Ch.3 Contact Resistance and Schottky Barriers

Dept. of Electrical Engineering, POSTECH

Prof. Rock-Hyun Baek

3.1 Introduction

- **All semiconductor devices have ‘contacts resistance’**
  - generally ‘metal-semiconductor’ contacts: in S/D region in Silicon device
  - also ‘semiconductor to semiconductor’ contacts: single crystal, polycrystalline, or amorphous

- **Schottky and Ohmic contacts**

① Schottky barrier devices
  - Schottky published theory in the 1930s
  - metal to semiconductor contact
  - distinctly non-linear current voltage characteristics

② Ohmic contacts (desired)
  - linear or quasi-linear current voltage characteristics
  - supplying the necessary devices current
  - small voltage drop is required

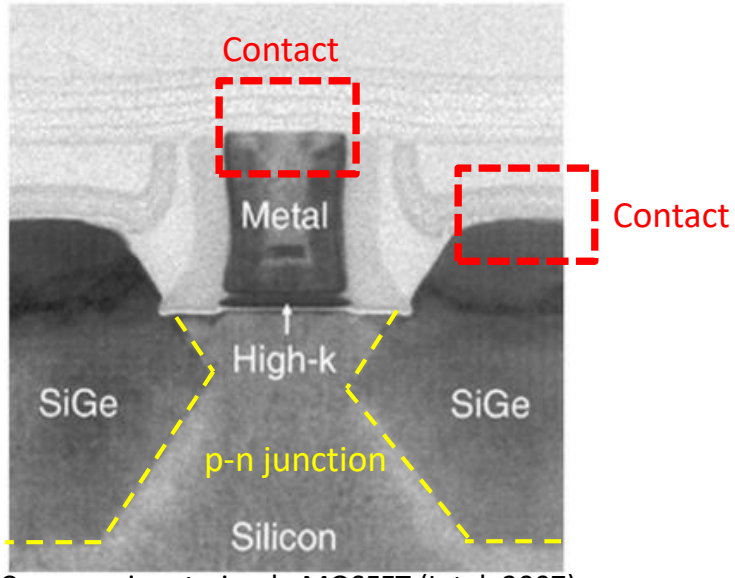

Compressive strained pMOSFET (Intel, 2007)

3.2 Energy band of Metal-Semiconductor contacts

- **Schottky model of the metal-semiconductor barrier**
  - work function: the energy difference between the ‘vacuum level’ and the ‘Fermi level’
  - metals of the appropriate work function to implement any one of the three barrier types

- **Schottky barrier height**

$$\emptyset_B = \emptyset_M - \chi \quad (3.1)$$

$\emptyset_B$: ideal schottky barrier height
$\emptyset_M$: metal work function
χ : electron affinity

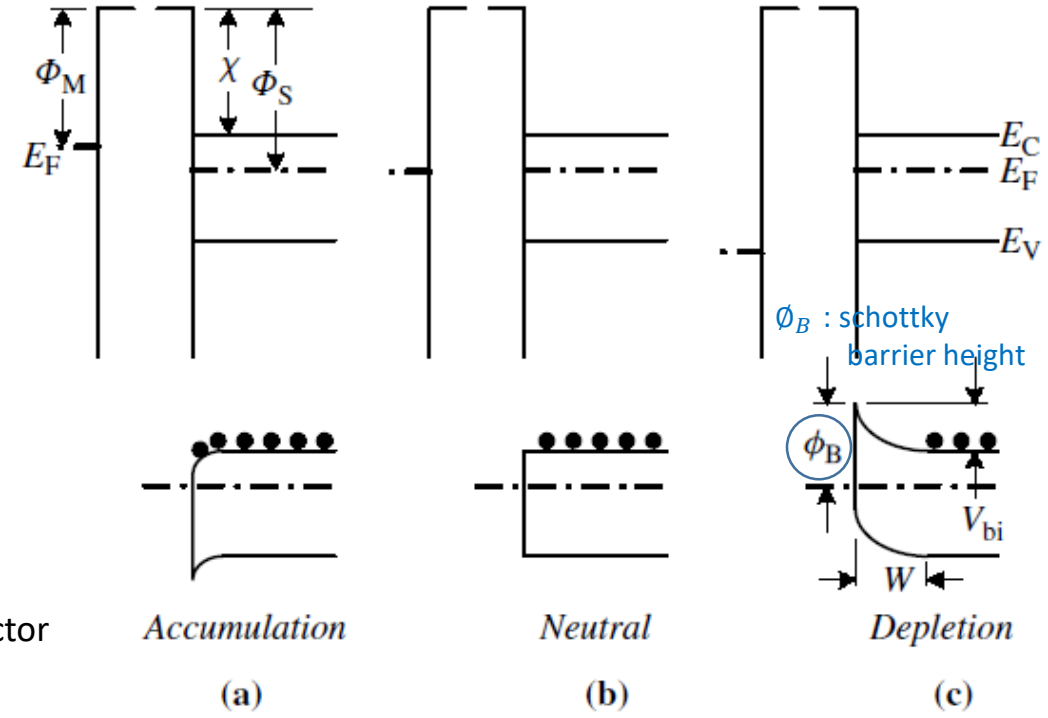

(a) Ohmic type contact
- accumulation
- least barrier
- e^- flows into or out of the semiconductor

(c) Depletion type contact
- depletion
- N substrate: $\emptyset_B = 2E_G/3$
- P substrate: $\emptyset_B = E_G/3$

Fig. 3.1 Metal-semiconductor contacts according to the simple Schottky model. The upper and lower parts of the figure show the metal-semiconductor system before and after contact, respectively.

3.2 Schottky barrier device in MOSFET (1/2)

- **Difficult to engineer an accumulation-type contact, i.e ohmic contact**
  - barrier heights independent of the various metal work function for the Ge, Si, GaAs, and other III-V
    → Fermi level pinning: Fermi level in the semiconductor is pinned at some energy in band gap
  - highly damaged regions should serve as good ohmic contact → not practical and not reproducible

- **Schottky barrier in conventional MOSFET**
  - **'barrier height'** is relatively independent of the doping density, but the **'barrier width'** does depend on the doping density
  - heavily doped semiconductor have narrow space-charge region width W (~ $N_D^{-1/2}$)
  - for metal-semiconductor contacts **narrow scr width**, **electrons can tunnel from the M to S and from the S to M**

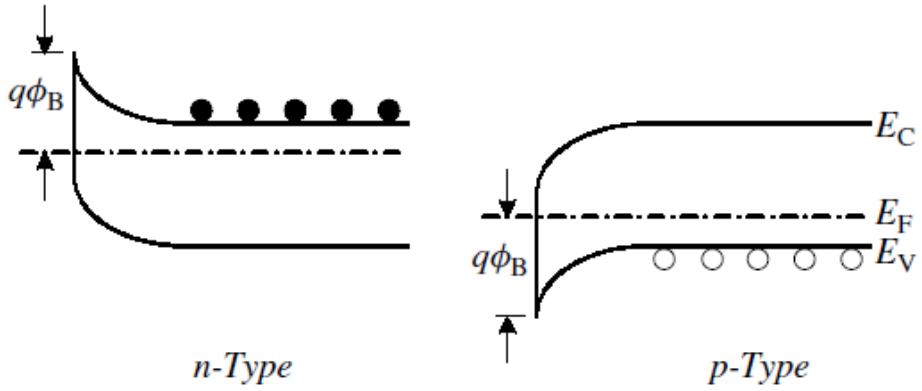

Fig. 3.2 Depletion-type contacts on *n*- and *p*-type substrates.

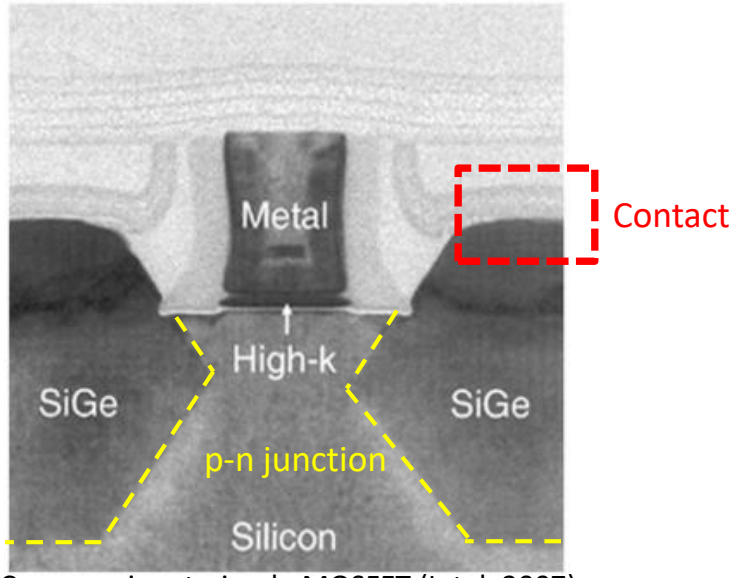

Compressive strained pMOSFET (Intel, 2007)

3.2 Schottky barrier device in MOSFET (2/2)

- **Generally only the semiconductor directly under the contact is heavily doped**
  - the region farther from the contact being less heavily doped
  - Source/Drain resistance is governed by contact resistance(R_{con}) and other resistances(R_{other})

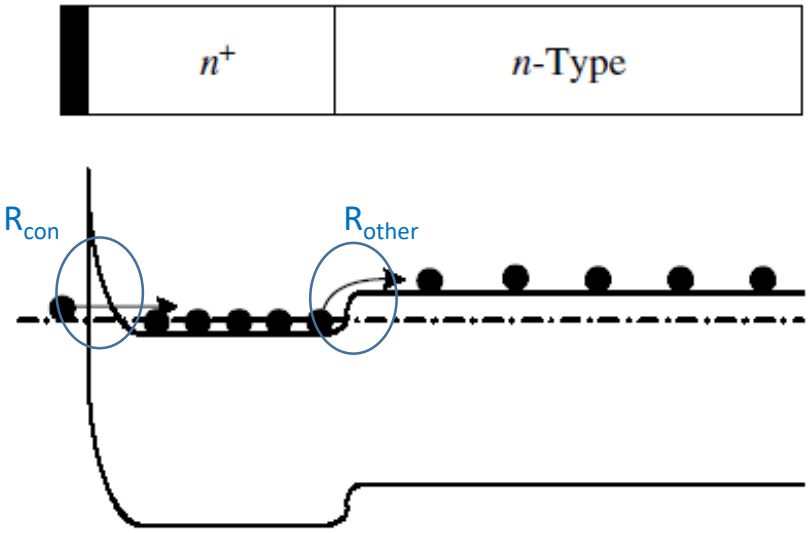

Fig. 3.5 A metal-n^+-n semiconductor contact band diagram.

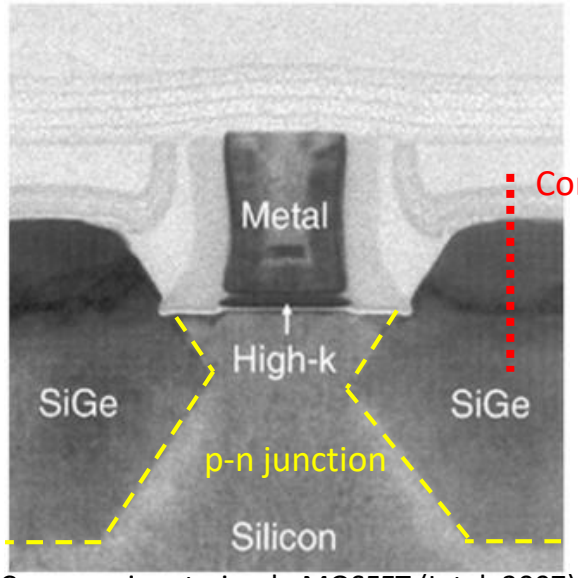

Compressive strained pMOSFET (Intel, 2007)

3.2 Conduction mechanism for M-to-S contact

- **Thermionic emission (TE)**
  - carriers thermally excited over the barrier

- **Thermionic-Field emission (TFE)**
  - carriers thermally excite to an energy where the barrier is sufficiently narrow for tunneling to take place

- **Field emission (FE)**
  - high doping density, the barrier is sufficiently narrow at or near the bottom of the conduction band for electron to tunnel directly

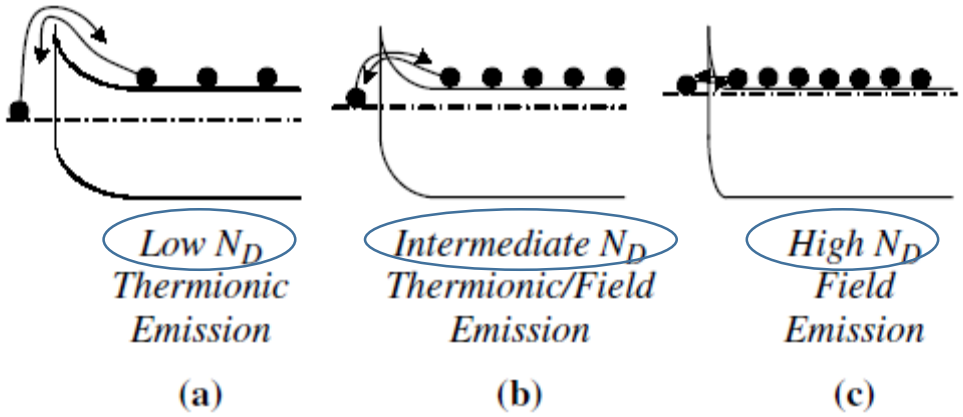

Fig. 3.3 Depletion-type contacts to *n*-type substrates with increasing doping concentrations. The electron flow is schematically indicated by the electrons and their arrows.

3.2 Characteristic energy, E_{00} [26]

- **Conduction mechanism can be differentiated by considering characteristic energy, E_{00}**

$$E_{00} = \frac{qh}{4\pi}\sqrt{\frac{N}{K_s\varepsilon_0 m^*_{tun}}} = 1.86 * 10^{-11}\sqrt{\frac{N\,(cm^{-3})}{K_s(m^*_{tun}/m)}}\,[\mathrm{eV}] \quad (3.2)$$

N : doping density
m^*_{tun}: tunneling effective mass
m: free electron mass

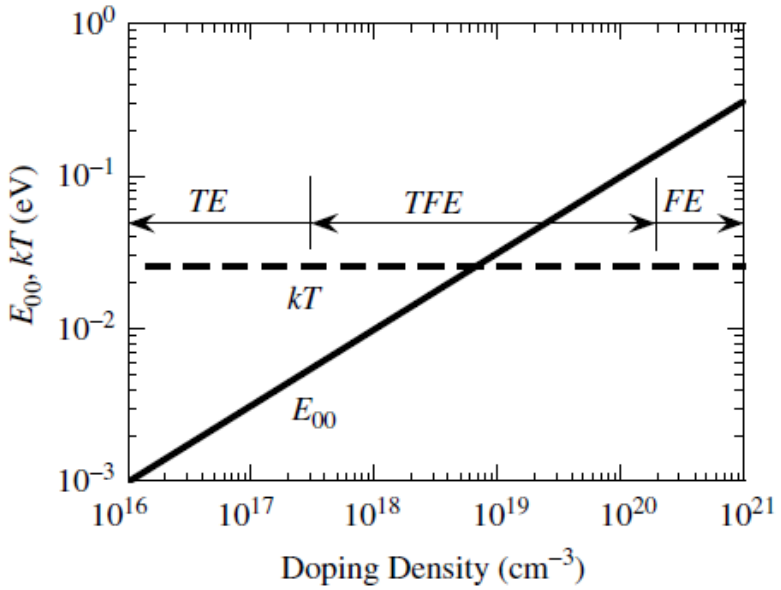

	Thermionic Emission	TFE	Field Emission
E_{00}	E_{00} < 0.5 kT	0.5 kT < E_{00} < 5 kT	E_{00} > 5 kT
N	N < 3E17 cm^{-3}	3E17 < N < 2E20 cm^{-3}	N > 2E20 cm^{-3}

Fig. 3.4 E_{00} and kT as a function of doping density for Si with $m^*_{tun}/m = 0.3$. $T = 300$ K.

3.3 Contact resistance

- **Metal-semiconductor contacts fall into two basic categories**
  - **current** flows either **'vertically'** or **'horizontally'** into the contact
  - vertical or lateral contacts can behave quite differently, because the **effective contact area may differ**

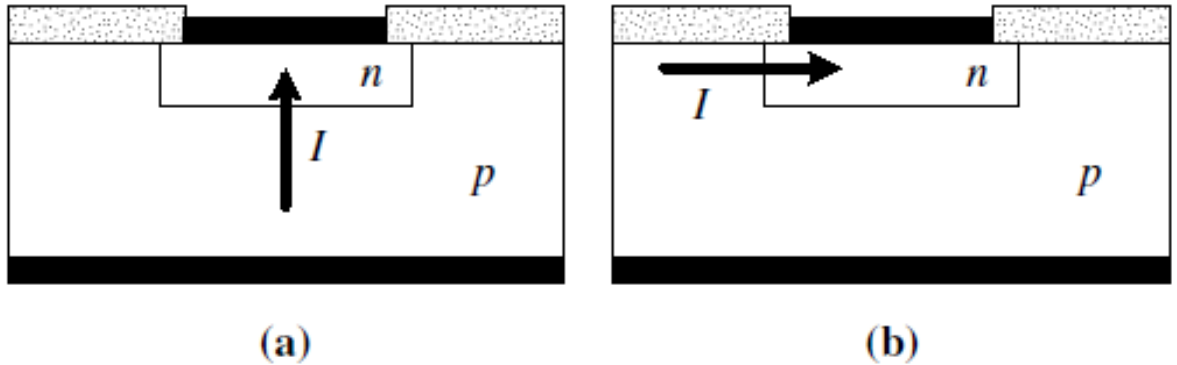

Fig. 3.6 (a) "Vertical" and (b) "horizontal" contact.

3.3 Uncertainty of contact resistance

- **Contact resistance includes…**
  - resistance of the metal-semiconductor contact, called the '**specific interfacial resistivity, ρ_i**'[10]
  - portion of the metal immediately above the M-S interface
  - portion of the semiconductor immediately below the M-S interface
  - current crowding effects
  - any interfacial oxide or other layer

$$R_T = 2R_m + 2R_c + R_{semi} \quad (3.3)$$

R_m : metal line resistance
R_c : contact resistance
R_{semi} : semiconductor resistance

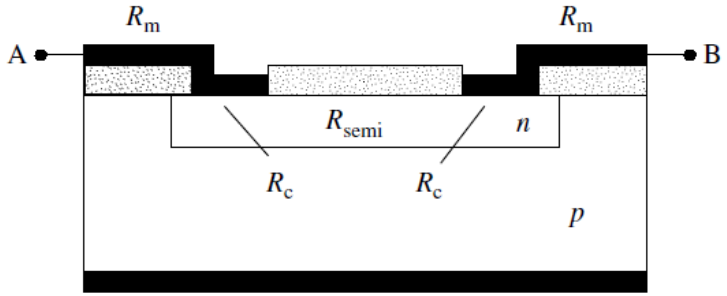

Fig. 3.7 A schematic diagram showing two contacts to a diffused semiconductor layer, with the metal resistance, the contact resistances and the semiconductor resistance indicated.

- **Contact resistance ρ_c is characterized by two quantities**
  - contact resistance (ohms)
  - contact resistivity, ρ_c (ohm·cm^2) or contact resistance

- **ρ_i vs. ρ_c**
  - ρ_i is the **theoretical** quantity referring to the metal-semiconductor **interface only**
  - ρ_c is the **measured** and **real** contact resistance including interface, above, and below the interface as well

3.3 Specific interfacial resistivity in different contact types

- Definition of **specific interfacial resistivity, ρ_i [Ωcm²]**

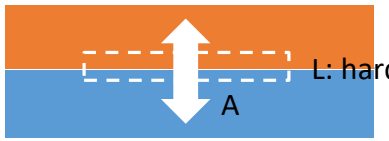

L: hard to define the exact length

$$J = f(V, \emptyset_B, N_D) \quad (3.4)$$

$$\rho_i = \left.\frac{\partial V}{\partial J}\right|_{V=0} \quad (3.5a)$$

$$\rho_i = \left.\frac{\partial V}{\partial J}\right|_{A\to 0} \quad (3.5b)$$

A: contact area [cm²]
→ plays a role in the behavior of the contact

- **Current density** of a metal-semiconductor contact dominated by '**thermionic emission**'

$$J = A^* T^2 e^{-q\emptyset_B/kT}\left(e^{qV/kT} - 1\right) \quad (3.6)$$

A*: 4pqk²m*/h³=120(m*/m) [A/cm²K²], Richardson's constant
m: free electron mass, m*: effective electron mass
T: absolute temperature

- ρ_i for thermionic emission using (3.5a) and (3.6)

Temperature dependent

$$\rho_i(TE) = \rho_1 e^{q\emptyset_B/kT}; \ \rho_1 = \frac{k}{qA * T} \quad (3.7)$$

- ρ_i for thermionic-field emission[9]

$$\rho_i(TFE) = C_1 \rho_1 e^{q\emptyset_B/E_0} \quad (3.8)$$

C_1, C_2: function of N_D, T, and $\emptyset_B$

$$E_0 = E_{00} \coth\left(E_{00}/kT\right) \quad (3.10)$$

- ρ_i for field emission[9]

$$\rho_i(FE) = C_2 \rho_1 e^{q\emptyset_B/E_{00}} \quad (3.9)$$

$$\rho_i(FE) \sim \exp\left(C_3/\sqrt{N}\right) \quad (3.11)$$

C_3: constant, N: doping density

Doping dependent

3.3 Scattered ρ_c with N_D and N_A

- **ρ_c vs. N_D and N_A**
  - there is considerable scatter, but a definite trend of lower specific contact resistivity with higher doping densities

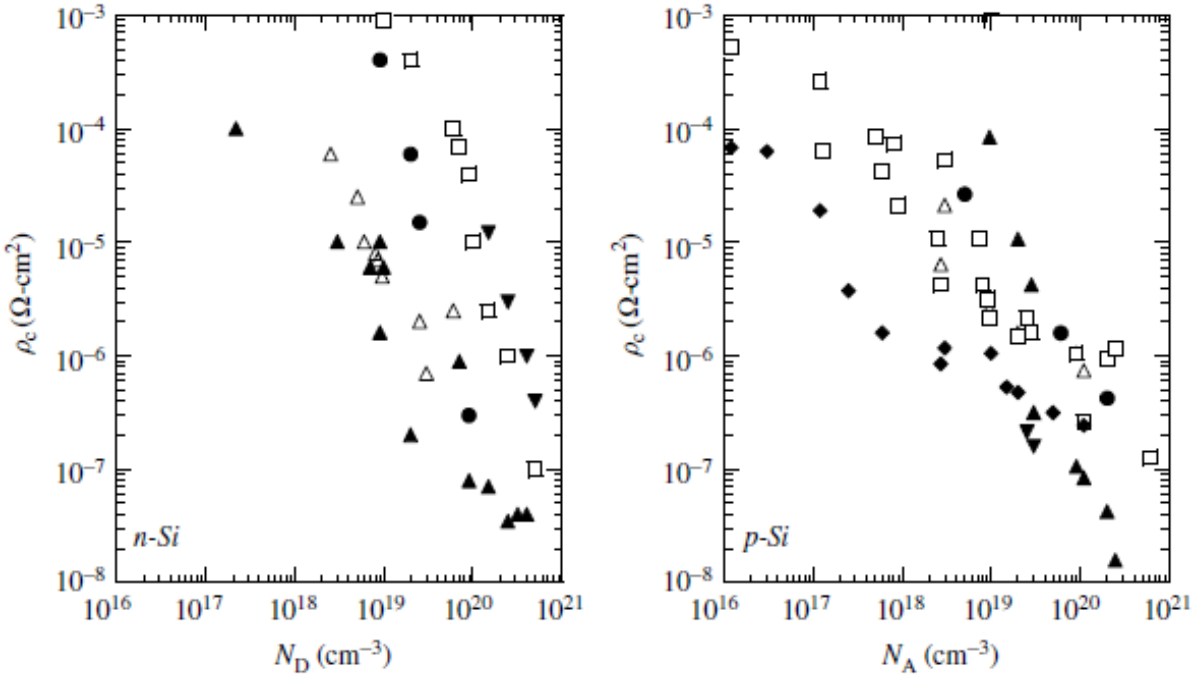

Fig. 3.8 Specific contact resistivity as a function of doping density for Si. The references for *n*-Si are given in ref. 35 and for *p*-Si in ref. 36.

3.4 Measurement technique of contact resistance

- **Contact resistance ρ_c measurement techniques, not ρ_i**
  - two-contact two-terminal
  - multiple-contact two-terminal
  - four-terminal, six-terminal

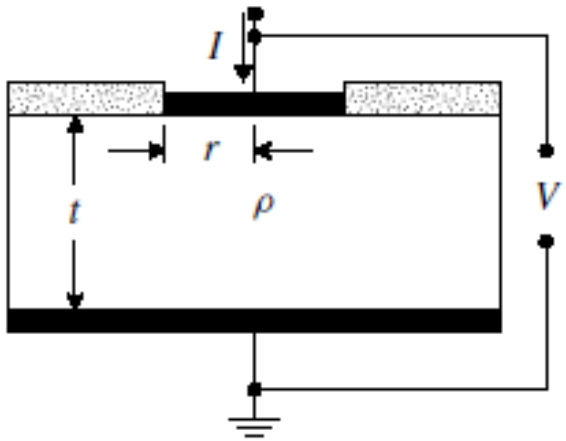

3.4.1 'Two-Contact Two-Terminal method'[41]

- the earliest method
- questionable accuracy if not properly executed
- R_c is determined by R_{sp}, but R_{sp} cannot be measured independently

- Spreading resistance equation for circular top contact

$$R_{sp} = \frac{\rho}{2\pi r}\arctan(2t/r) \quad (3.13)$$

$$R_{sp} = C\frac{\rho}{4r} \quad for \quad 2t \gg r \quad (3.14)$$

r : radius of top contact
ρ : semiconductor resistivity
t: thickness

C: correction factor

- Contact resistance

target

$$R_c = \frac{\rho_c}{A_c} = \frac{\rho_c}{\pi r^2} \quad (3.15)$$

target 0

$$R_T = R_c + R_{sp} + R_{cb} + R_p \quad (3.12a)$$

R_c : the contact resistance of the top contact
R_{sp}: the spreading resistance in the semiconductor directly under the contact
R_{cb}: the contact resistance of the bottom contact (negligible)
R_p: the probe or wire resistance

3.4.1 Common lateral structure

- **Lateral structure**
  - more commonly implemented
  - confining the current to the n-island
  - two contacts separated by the spacing *d*
  - generally contact width Z differs from W, Z < W

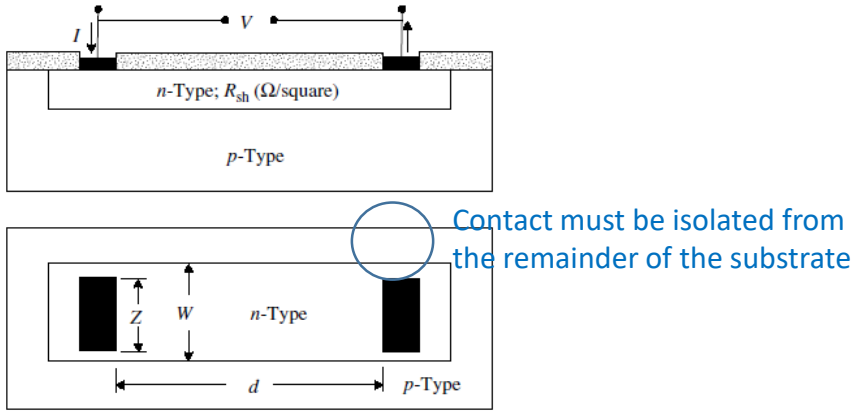

Fig. 3.11 A lateral two-terminal contact resistance structure in cross section and top view.

$$R_T = R_{sh}d/W + R_d + R_w + 2R_c \quad (3.16)$$

R_{sh} : the sheet resistance of the n-layer
R_d: the resistance due to 'current crowding' under the contacts
R_w: the contact width correction if Z <W
R_c: the contact resistance, assuming two identical contact

- **Contact chain or contact string**
  - commonly used for process control or monitoring

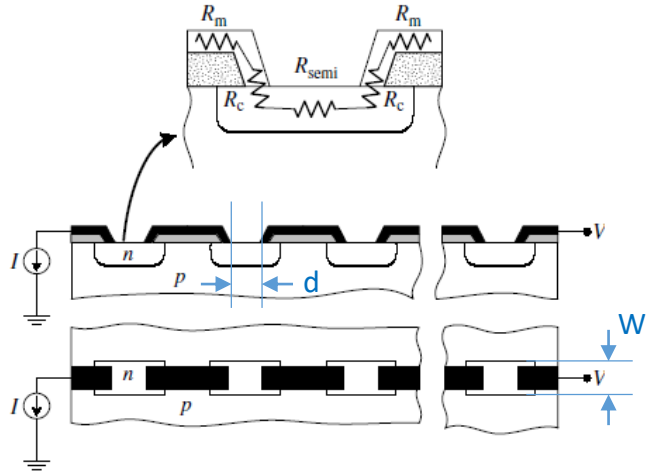

Fig. 3.12 A contact string test structure; cross section and top view.

- Contact string consisting of *N* islands and *2N* contacts
  - spacing d and width W
  - neglecting the metal resistance, R_m

$$R_T = \frac{NR_{sh}d}{W} + 2NR_c \quad (3.17)$$

3.4.2 Multiple-Contact Two-Terminal Methods

- **'Multiple-contact Two-terminal methods'**
  - to overcome the deficiencies of the two-contact, two-terminal method
  - ρ_c cannot be directly extracted from the two resistance measurement
  - assuming 'three identical contacts'
  - not necessary of bulk resistance or layer sheet resistance R_{sh}

$$R_{Ti} = \frac{R_{sh} d_i}{W} + 2R_c \qquad (3.18)$$

target

$$R_c = \frac{R_{T2} d_1 - R_{T1} d_2}{2(d_1 - d_2)} \qquad (3.19)$$

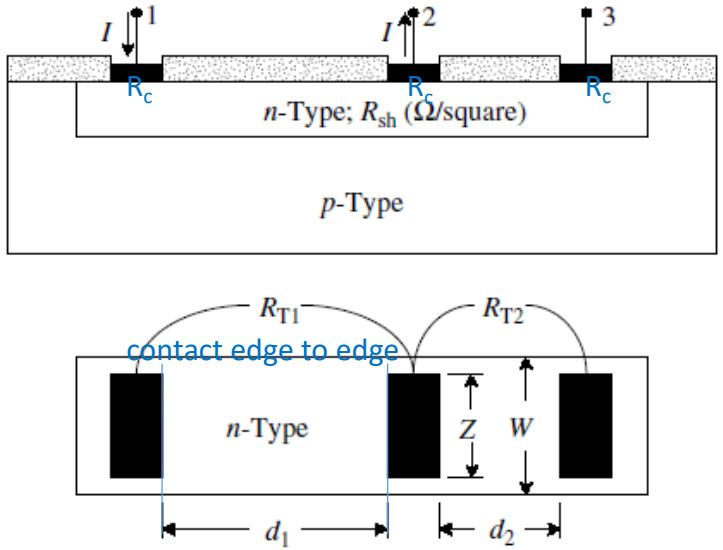

Fig. 3.13 Multiple-contact, two-terminal contact resistance test structure. The contact width and length are Z and L and the diffusion width is W.

Transmission Line Model (TLM)

- **'Transmission Line Model'**
  - to take **'current crowding'** into account and to extract 'specific contact resistivity, ρ_c'
  - obtaining both the 'semiconductor sheet resistance, R_{sh}' and the 'contact resistance, R_c'

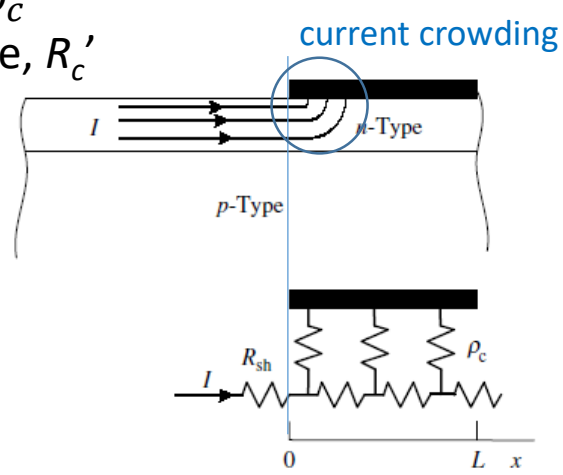

Fig. 3.14 Current transfer from semiconductor to metal represented by the arrows. The semiconductor/metal contact is represented by the ρ_c-R_{sh} equivalent circuit with the current choosing the path of least resistance.

- When current flows from S-to-M,
  - potential distribution[54] under the contact is determined by ρ_c and R_{sh}

$$V(x) = \frac{I\sqrt{R_{sh}\rho_c}}{Z}\frac{\cosh[(L-x)/L_T]}{\sinh(L/L_T)} \qquad (3.20)$$

L: the contact length
Z: the contact width
I: the current flowing into the contact

- **Transfer length, L_T**
  - 1/e(~0.37) distance of the voltage curve
  - distance over which most of the current transfers from the S-into-M or M-into-S

$$L_T = \sqrt{\rho_c/R_{sh}} \qquad (3.21)$$

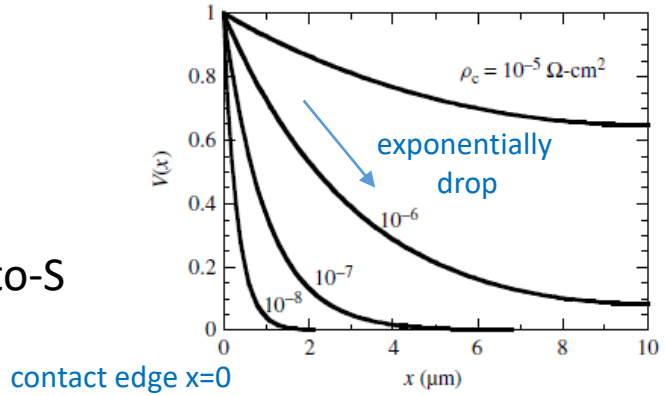

Fig. 3.15 Normalized potential under a contact versus x as function of ρ_c, where $x = 0$ is the contact edge. $L = 10$ μm, $Z = 50$ μm, $R_{sh} = 10$ Ω/square.

Transfer length, L_T

- **'Transfer length limitation' by specific contact resistance, ρ_c**
  - ex) when ρ_c=10^{-6} Ωcm^2, then transfer length L_T~1μm
    contact area longer than 1μm is inactive during current transfer
  - for further S/D scaling, less transfer length is necessary

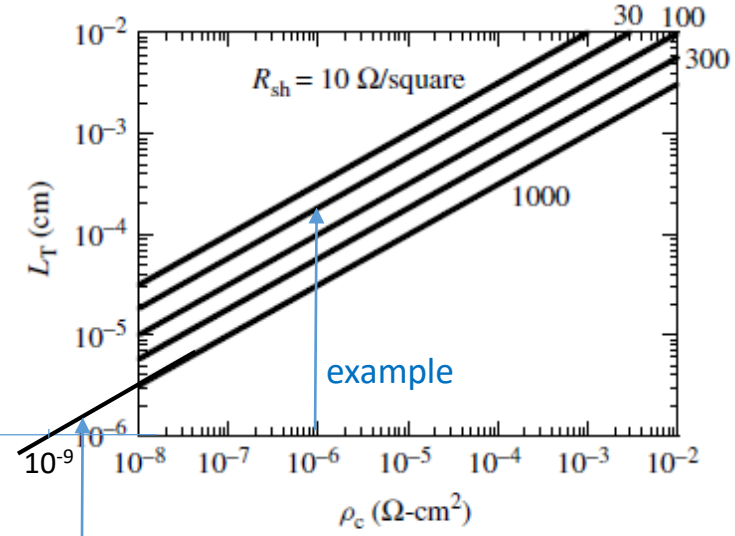

Fig. 3.16 Transfer length as a function of specific contact resistivity and semiconductor sheet resistance.

Current technology (17')

TLM configurations: CFR, CER, CBKR

Where to measure the Voltage in contact area ?

- **CFR:** ‘Contact Front Resistance’ test structure
- **CER:** ‘Contact End Resistance’ test structure
- **CBKR:** ‘Cross Bridges Kelvin Resistance’ test structure

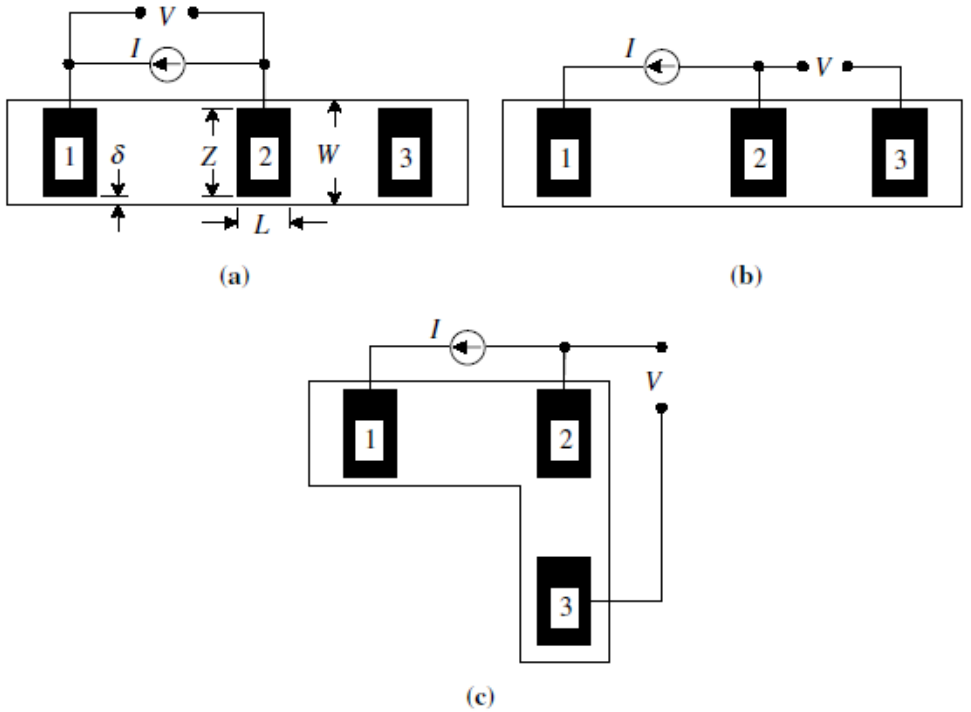

Fig. 3.17 (a) Conventional contact resistance test structure, (b) contact end resistance test structure, and (c) cross bridge Kelvin resistance test structure.

Contact Front Resistance

- **R_c of contact front edge**
  - using (3.20) with V measured between contact 1 and 2 at x=0 (contact edge)
  - assuming Z=W, (3.22) does not consider the current flow around the contacts

measured

$$R_{cf} = \frac{V}{I} = \frac{\sqrt{R_{sh}\rho_c}}{Z}\coth(L/L_T) = \frac{\rho_c}{L_T Z}\coth(L/L_T) \qquad (3.22)$$

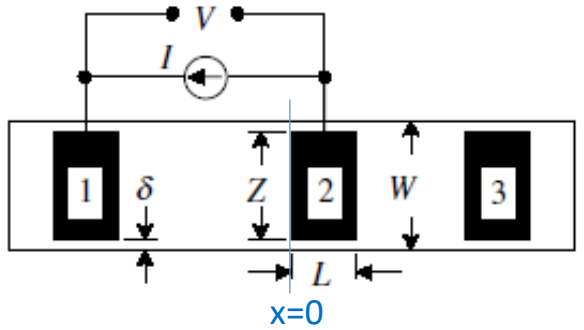

① for $L \le 0.5\ L_T$, $\coth(L/L_T) \approx L/L_T$

$$R_c \approx \frac{\rho_c}{LZ} \qquad (3.23a)$$

effective contact area, $A_{c,eff}=LZ$, actual contac

② for $L \ge 1.5\ L_T$, $\coth(L/L_T) \approx 1$

$$R_c \approx \frac{\rho_c}{L_T Z} \qquad (3.23b)$$

effective contact area $A_{c,eff}=L_T Z$

Determined by L

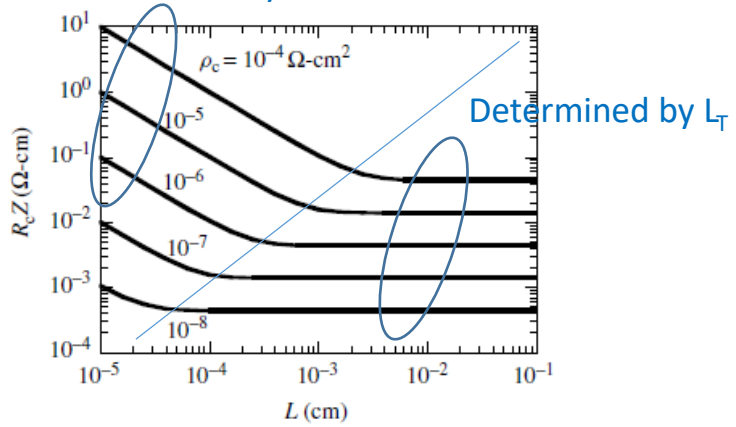

Determined by L_T

Fig. 3.18 Front contact resistance–contact width product as a function of contact length and specific contact resistivity for $R_{sh} = 20$ Ω/square and $R_{sm} = 0$.

ex) R_{sh}=20Ω/square and ρ_c=10^{-7} Ωcm² → transfer length L_T=0.7μm
for contact length L=10 μm and width Z=50 μm → actual contact area is **LZ**=5x10^{-6} cm², **L_TZ**=0.35x10^{-6} cm²

current density is 5/0.35=14 times higher, reliability problem by contact degradation

Contact End Resistance

- **R_c of contact end edge**
  - voltage is measured between contacts 2 and 3, current flowing from 1 to 2
  - voltage is now measured at x=L, and (3.20) can be changed

measured

$$R_{ce} = \frac{V}{I} = \frac{\sqrt{R_{sh}\rho_c}}{Z}\frac{1}{\sinh(L/L_T)} = \frac{\rho_c}{L_T Z}\frac{1}{\sinh(L/L_T)} \qquad (3.24)$$

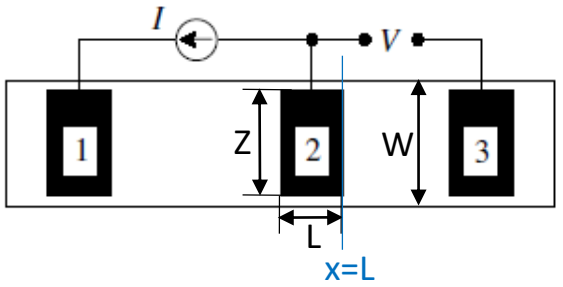

① for short contact (L is short), R_{ce} is sensitive to contact length variations
② for long contact (L>> L_T), R_{ce} becomes very small and the accuracy is limited by instrumentation

- R_{ce}/R_{cf} becomes very small for L>> L_T

$$\frac{R_{ce}}{R_{cf}} = \frac{1}{\cosh(L/L_T)} \qquad (3.25)$$

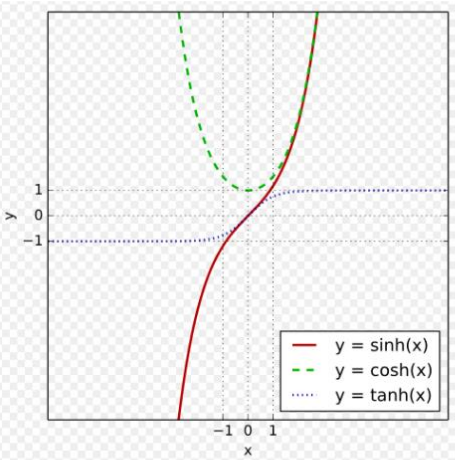

- Above we assumed Z=W, but usually Z < W

  ex) experiments with Z=5 μm, 10 μm < W < 60 μm shows that that CER to give erroneously high ρ_c

To avoid the error, test structure should meet the conditions: L ≤ L_T, Z >> L, and δ << Z

Cross Bridge Kelvin Resistance (CBKR)

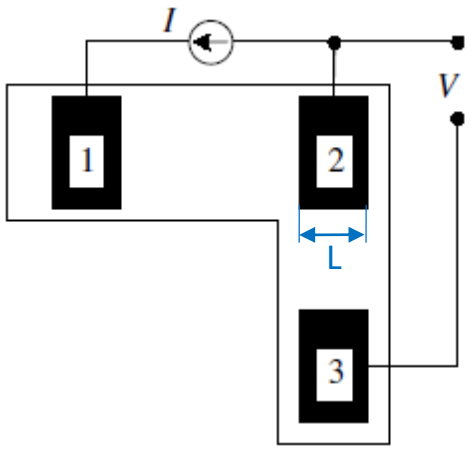

- **R_c of whole range from x=0 to x=L**
  - voltage contact 3 is located at the side of contact 2

- The measured voltage is the linear average of the potential over the contact length, L

- Integrating V(x) of (3.20)

$$V = \frac{1}{L}\int_0^L V(x)dx \qquad (3.26)$$

- contact resistance

$$R_c = \frac{V}{I} = \frac{\rho_c}{LZ} \qquad (3.27)$$

Circular contact resistance (circular TLM)

- Advantages: avoiding the problem of W≠Z, not necessary to isolate the layer
- The total resistance between the internal and the external contacts[60]

$$R_T = \frac{R_{sh}}{2\pi}\left[\frac{L_T}{L}\frac{I_0(L/L_T)}{I_1(L/L_T)} + \frac{L_T}{L+d}\frac{K_0(L/L_T)}{K_1(L/L_T)} + \ln\left(1+\frac{d}{L}\right)\right] \quad (3.28)$$

- Simplified R_T at $L >> 4L_T$, I_0/I_1 and $K_0/K_1 \sim 1$

$$R_T = \frac{R_{sh}}{2\pi}\left[\frac{L_T}{L} + \frac{L_T}{L+d} + \ln\left(1+\frac{d}{L}\right)\right] \quad (3.29)$$

- Simplified R_T at $L >> d$ at Fig.3.19(b),

$$R_T = \frac{R_{sh}}{2\pi L}(d+2L_T)C \quad (3.30)$$

$$C = \frac{L}{d}\ln\left(1+\frac{d}{L}\right) \quad (3.31)$$

C: correction factor
- necessary when *d* increase (Fig.3.19(b))

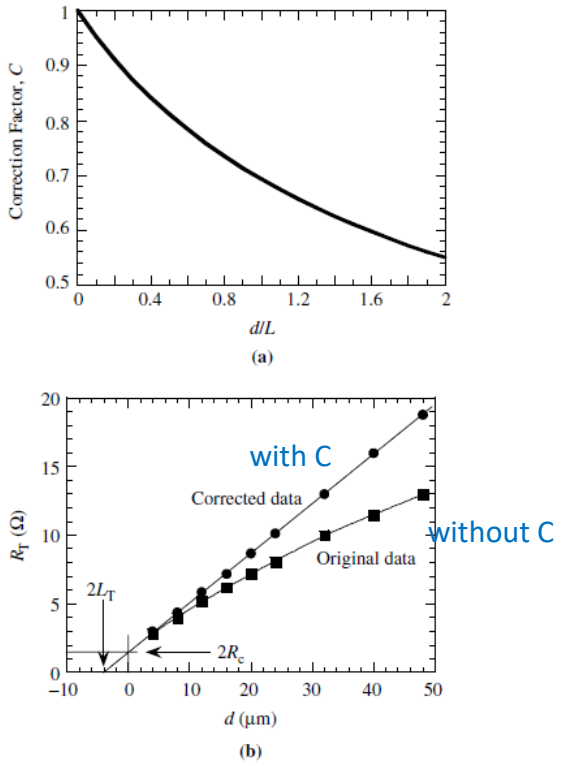

Fig. 3.20 (a) Correction factor C versus d/L ratio for the circular transmission line method test structure, (b) total resistance for the circular TLM test structure before and after data correction. $R_C = 0.75$ ohms, $L_T = 2$ μm, $\rho_c = 4 \times 10^{-6}$ ohm-cm^2, $R_{sh} = 110$ ohms/square. Data courtesy of J.H. Klootwijk and C.E. Timmering, Philips Research Labs.

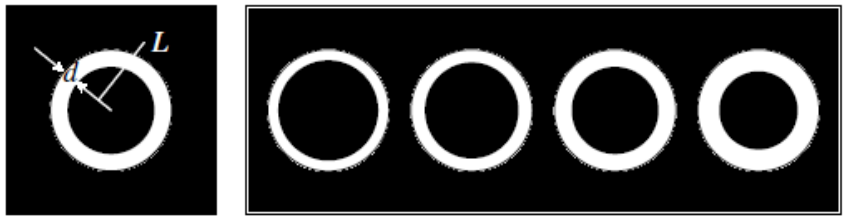

Fig. 3.19 Circular contact resistance test structure. The dark regions represent metallic regions. Spacing d and radius L are shown in (a).

Transfer Length Method (TLM) (1/2)

- Advantages: solving the difficulty of deciding where to measure the voltage in Fig. 3.17
- In this TLM, consisting of more than three contacts

- Fig.3.21(b) is more general,
  when voltage is measured between contacts 1 and 4, the current flow may be perturbed by contacts 2 and 3

  ① L << L_T, current does not penetrate into the contact metal and 2/3 contact have not effect on the measurement
  ② L >> L_T, current does flow into the metal and the contact can be thought of as two contacts,
  each of length L_T joined by a metallic conductor

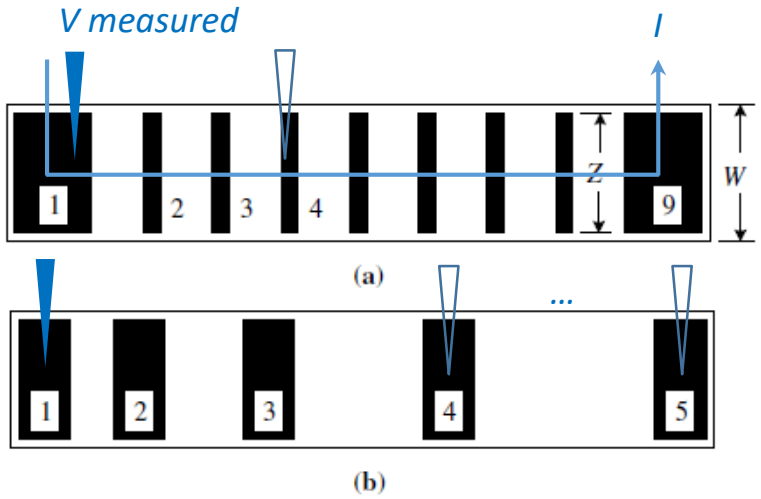

Fig. 3.21 Transfer length method test structures.

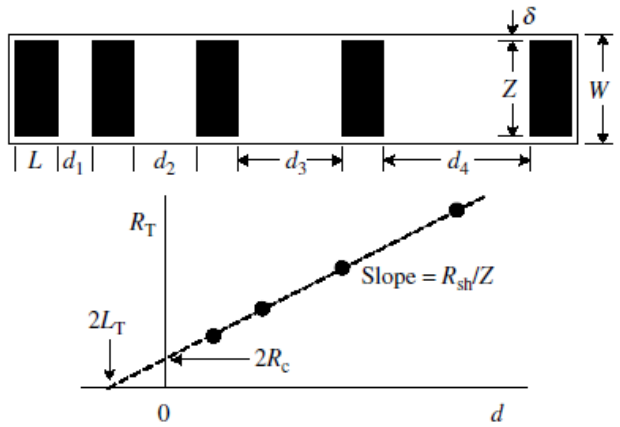

Fig. 3.22 A transfer length method test structure and a plot of total resistance as a function of contact spacing, d. Typical values might be: $L = 50$ μm, $W = 100$ μm, Z-$W = 5$ μm (should be as small as possible), $d \approx 5$ to 50 μm.

Transfer Length Method (TLM) (2/2)

- Using contact with **L ≥ 1.5 L_T** and **'front contact resistance measurement'** of structure in Fig.3.21(b) $R_c \approx \frac{\rho_c}{L_T Z}$ $(3.23b)$
- Total resistance between any two contact

$$R_T = \frac{R_{sh} d}{Z} + 2R_c \approx \frac{R_{sh}}{Z}(d + 2L_T) \quad (3.33)$$

$$L_T = \sqrt{\rho_c / R_{sh}} \quad (3.21)$$

similar to (3.32) with the contact peripheral length '$2\pi L$' replaced by contact width 'Z'

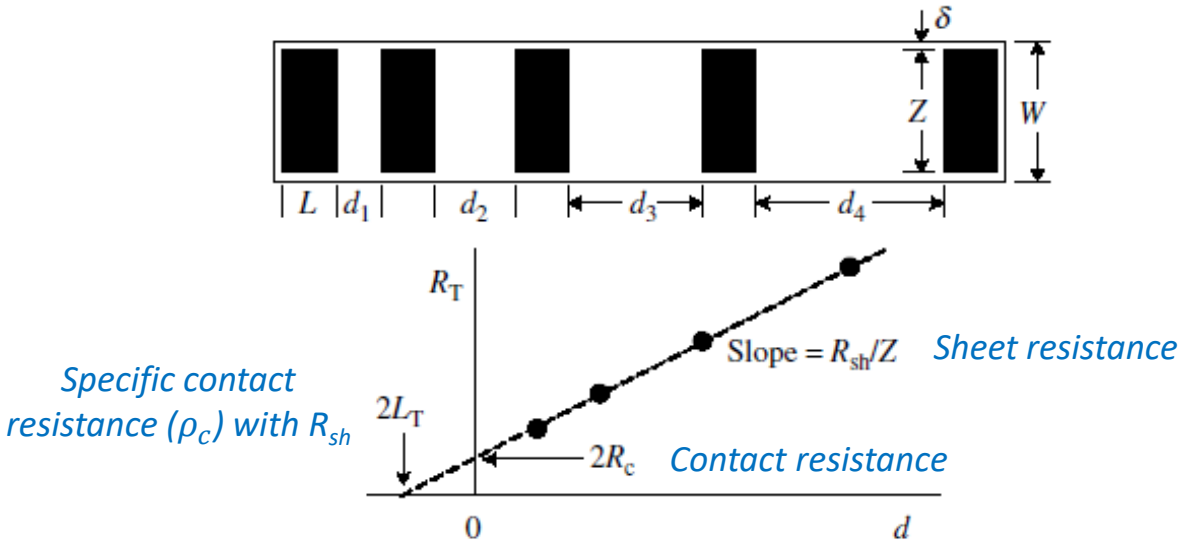

Fig. 3.22 A transfer length method test structure and a plot of total resistance as a function of contact spacing, d. Typical values might be: $L = 50$ μm, $W = 100$ μm, Z-$W = 5$ μm (should be as small as possible), $d \approx 5$ to 50 μm.

Improved Transfer Length Method (TLM) (1/2)

① Considering 'alloyed and silicided contacts'[66]

R_{sh}: sheet resistance
R_{sk}: sheet resistance under the contact
$L_{Tk}=(\rho_c/R_{sk})^{1/2}$

modified front contact resistance

$$R_{cf} = \frac{\rho_c}{L_{Tk}Z}\coth(L/L_{Tk}) \qquad (3.34)$$

total resistance

Known (3rd)

$$R_T = \frac{R_{sh}d}{Z} + 2R_C \approx \frac{R_{sh}d}{Z} + \frac{2R_{sk}L_{Tk}}{Z} = \frac{R_{sh}}{Z}[d + 2(R_{sk}/R_{sh})L_{Tk}] \quad (3.35)$$

modified end contact resistance

Known (2nd) Known (1st)

$$R_{ce} = \frac{\sqrt{R_{sk}\rho_c}}{Z\sinh(L/L_{Tk})} = \frac{\rho_c}{ZL_{Tk}\sinh(L/L_{Tk})};\ \frac{R_{ce}}{R_{cf}} = \frac{1}{\cosh(L/L_{Tk})} \quad (3.36)$$

② Considering 'metal resistance'[68-69] (universal form)

$$R_{cf} = \frac{\rho_c}{L_{Tm}Z(1+\alpha)^2}\left[(1+\alpha^2)\coth(L/L_{Tm}) + \alpha\left(\frac{2}{\sinh(L/L_{Tm})} + \frac{L}{L_{Tm}}\right)\right] \quad (3.37)$$

$\alpha=R_{sm}/R_{sk}$, R_{sm}: metal sheet resistance, $L_{Tm}=[\rho_c/(R_{sm}+R_{sk})]^{1/2}=L_{Tk}/(1+\alpha)^{1/2}$

for $R_{sm}=0$, (3.37) → (3.24)
for $R_{sm}=0$ and $R_{sk}=R_{sh}$, (3.37) → (3.22)

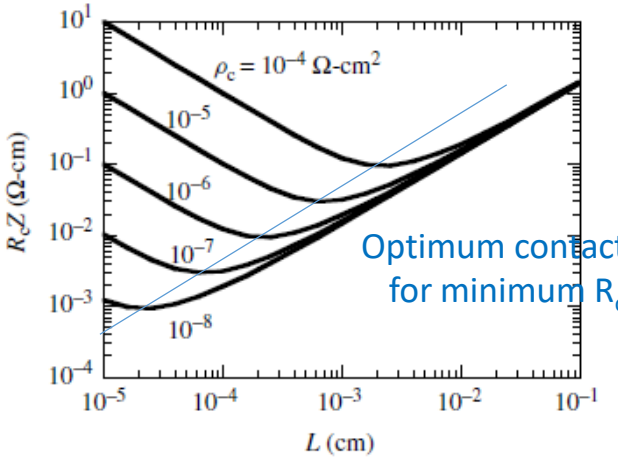

Fig. 3.23 Front contact resistance–contact width product as a function of contact length and specific contact resistivity for $R_{sk} = 20$ Ω/square and $R_{sm} = 50$ Ω/square.

Improved Transfer Length Method (TLM) (2/2)

③ Considering gap δ=W-Z[71]

$$R' = 2R_{ce} + \frac{(R_T(\delta \neq 0) - 2R_{ce})R_p}{R_p - R_T(\delta \neq 0) - 2R_{ce}} \qquad (3.38)$$

R_{ce}: contact end resistance
R_T: measured resistance
R_P: parallel 'strip' resistance

Different intercepts for the uncorrected lines
→ incorrect R_c, L_T, and ρ_c

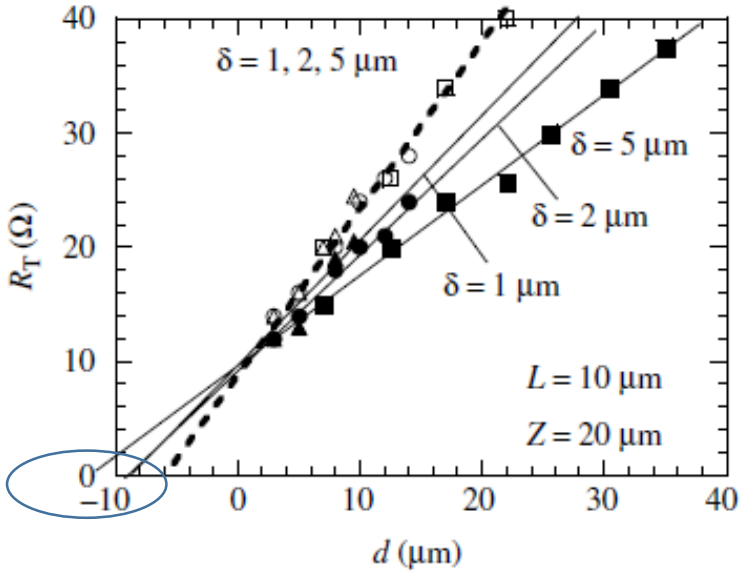

Fig. 3.24 Uncorrected (solid points and lines) and corrected (open points and dashed line) total resistance versus spacing d for Au/Ni/AuGe/n-GaAs contacts annealed at 400°C for 20 s. Reprinted after ref. 72 by permission of IEEE (© 2002, IEEE).

3.4.3 Four-Terminal Contact Resistance Method (1/3)

'Cross-Bridge Kelvin Resistance (CBKR) method'

- Advantages: not necessary of 'semiconductor bulk resistivity' or 'sheet resistance'

- In principle,
  ρ_c is measured without being affected by the underlying semiconductor or the contacting metal conductor

- Current flows between contacts 1 and 2
  Voltage is measured between contacts 3 and 4

  - using high input impedance voltmeter
  - little current flow between contacts 3 and 4
  - V_4 is the same as V where is directly under contact 2/3
    → V_{34} is solely due to the voltage drop across the interface

$$R_c = \frac{V_{34}}{I} \quad (3.39)$$

$$\rho_c = R_c A_c \quad (3.40)$$

A_c: contact area

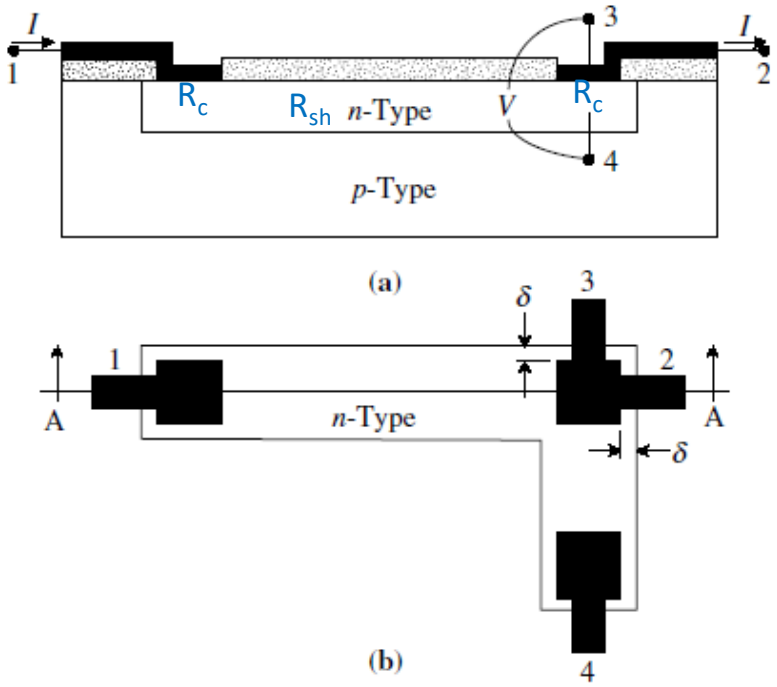

Fig. 3.25 A four-terminal or Kelvin contact resistance test structure. (a) Cross section through section A–A, (b) top view of the structure.

3.4.3 Four-Terminal Contact Resistance Method (2/3)

- **Lateral current crowding** in real contact
  - δ> 0 to consider 'diffusion layer misalignment' and 'lateral dopant diffusion'

$$R_k(modified\ Rc) = \frac{\rho_c + \sqrt{\rho_c R_{sh}} L_1 \coth(L/L_T) + 0.5\, R_{sh} L_1^2 + \sqrt{\rho_c R_{sh}} L_2 / \sinh(L/L_T)}{(L + L_1 + L_2)W} \quad (3.41)$$

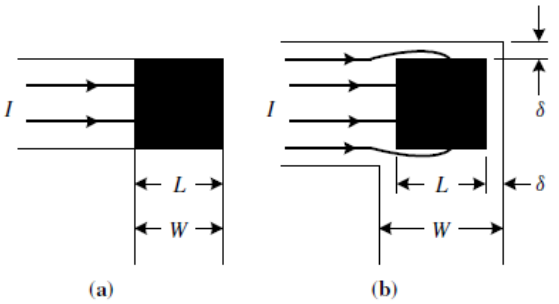

Fig. 3.26 Four-terminal contact resistance test structures. (a) Ideal with only lateral current flow, (b) showing current flowing into and around the contact. The black area is the contact area.

- **Larger δ, higher R_k**

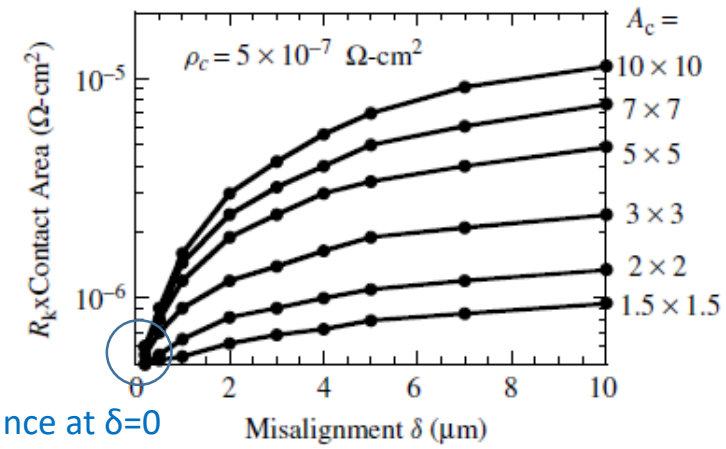

True resistance at δ=0

- **L_1 and L_2 misalignment effect on R_k**

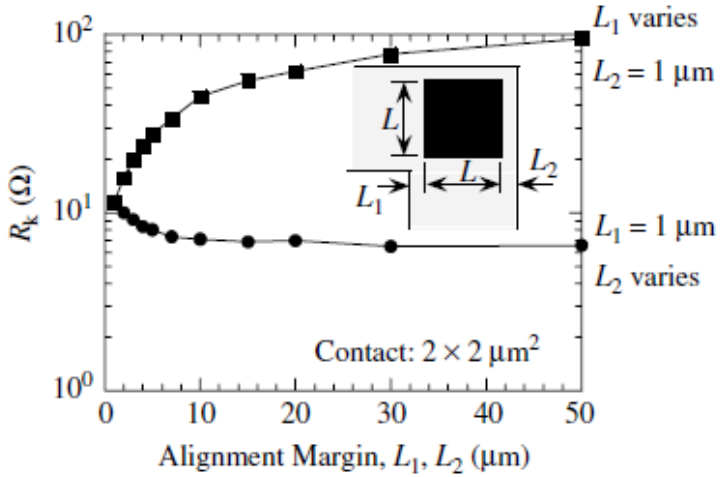

Fig. 3.27 Apparent contact resistance multiplied by the contact area versus misalignment δ. The contact areas are given on the right side of the figure. Under the contact: Arsenic implant, 2×10^{15} cm^{-2}, 50 keV, annealed at 1000°C, 30 s. Contact metal: Ti/TiN/Al/Si/Cu. Adapted from ref. 80.

Fig. 3.28 Dependence of contact resistance on misalignment dimensions L_1 and L_2. Under the contact: Arsenic implant, 2×10^{15} cm^{-2}, 50 keV, annealed at 1000°C, 30 s. Contact metal: Ti/TiN/Al/Si/Cu. Adapted from ref. 80.

3.4.3 Four-Terminal Contact Resistance Method (3/3)

- **Modified CBKR**
  - using very long contact length L=500 μm
  - by extrapolating the data to zero tap spacing, the true resistance is obtained

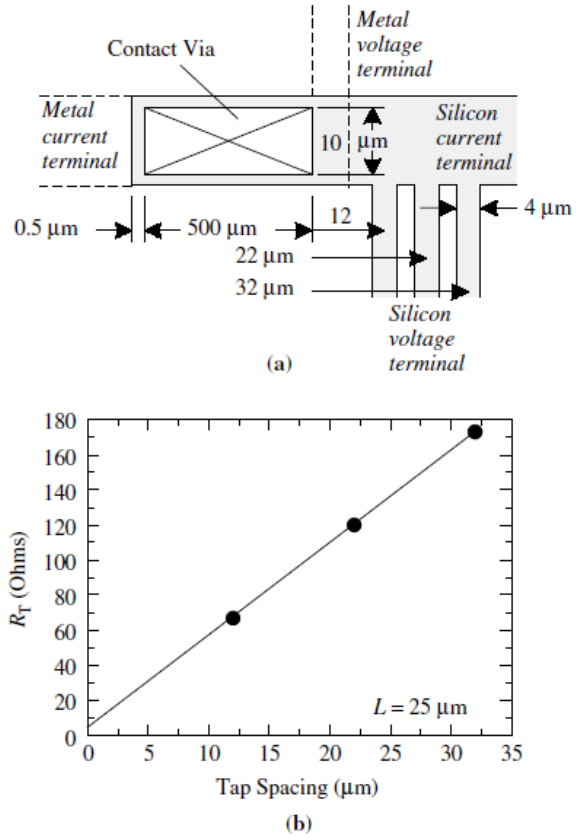

Fig. 3.29 (a) Modified Kelvin contact resistance "tapped" test structure and (b) resistance versus tap spacing. After ref. 80.

3.5 Schottky Barrier Height

- **Thermionic current-voltage** (not excessive doping in Semiconductor)

$$I = \underbrace{AA^*T^2 e^{-\frac{q\phi_B}{kT}}}_{I_s}\left(e^{qV/nkT} - 1\right) = I_{s1}e^{-\frac{q\phi_B}{kT}}\left(e^{qV/nkT} - 1\right)$$
$$= I_s\left(e^{qV/nkT} - 1\right) \qquad (3.43)$$

A: diode area, n: ideal factor (including unknown factors)
A*: $4\pi qk^2m^*/h^3=120(m^*/m)$ [A/cm²K²], Richardson's constant

- From (3.43), $I/\left(1 - e^{-qV/nkT}\right) = I_s e^{qV/nkT}$

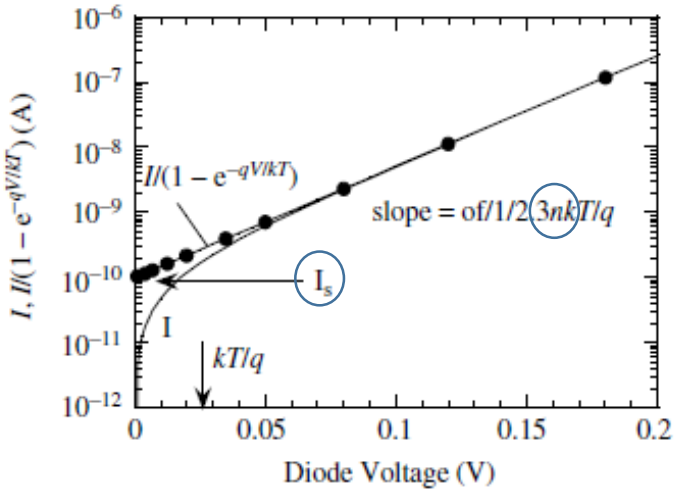

Fig. 3.37 Two ways of plotting current-voltage for a Schottky diode. Reprinted with permission from *Journal of Applied Physics*, **69**, 7142–7145, May 1991. Copyright American Institute of Physics.

ϕ_{B0}: ideal barrier height
ϕ_B: actual barrier height due to image force barrier lowering
V_{bi}: built-in potential

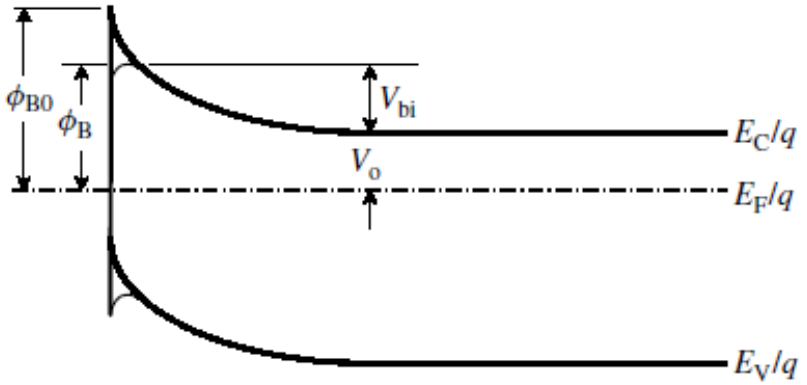

Fig. 3.36 Schottky barrier potential band diagram.

TABLE 3.1 Experimental A^* Values.

Semiconductor	A^* (A/cm² · K²)	Ref.
n-Si	112 (±6)	95
p-Si	32 (±2)	95
n-GaAs	4–8	96
n-GaAs	0.41 (±0.15)	97
p-GaAs	7 (±1.5)	97
n-InP	10.7	109

3.5.1 $\emptyset_B$ from Current-Voltage

- **ϕ_B calculation using I-V**
  - barrier height φ_B is most commonly calculated from the current I_s
  - forward bias condition

$$\emptyset_B = \frac{kT}{q}\ln\left(\frac{AA^*T^2}{I_s}\right) \qquad (3.45)$$

A(area)= 3.1x10^{-3} [cm^2]
A*=110 [A/cm^{2}K^2] for n-Si
n=1.05
I_s=5x10^{-6} [A]

ϕ_B(I-V)=0.58 V

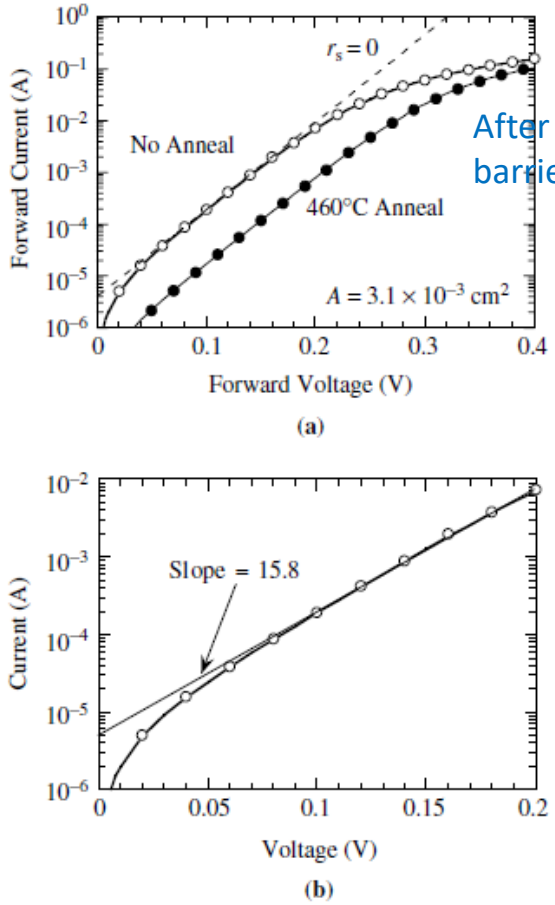

After annealing at 460°C, barrier height increases

Fig. 3.38 (a) Current-voltage characteristics of a Cr/*n*-Si diode as deposited and annealed at 460°C measured at room temperature, (b) enlarged portion of (a). Courtesy of F. Hossain, Arizona State University.

3.5.2 $\emptyset_B$ from Current-Temperature

- For V>> kT/q, (3.43) can be written as

$$\ln(I/T^2) = \ln(AA^*) - q(\emptyset_B - V/n)/kT \qquad (3.46)$$

- **ϕ_B calculation using Current-Temperature**
  - differentiating (3.46) by (1/T)
  - forward bias condition

Forward bias

$$\emptyset_B = \frac{V_1}{n} - \frac{k}{q}\frac{d[\ln(I/T^2)]}{d(1/T)} = \frac{V_1}{n} - \frac{2.3k}{q}\frac{d[\log(I/T^2)]}{d(1/T)} \qquad (3.47)$$

slope

V_1=0.2 [V]
Slope d[log(I/T^2)]/d(1000/T)=-1.97
n=1.05

ϕ_B(I-T)=0.59 V

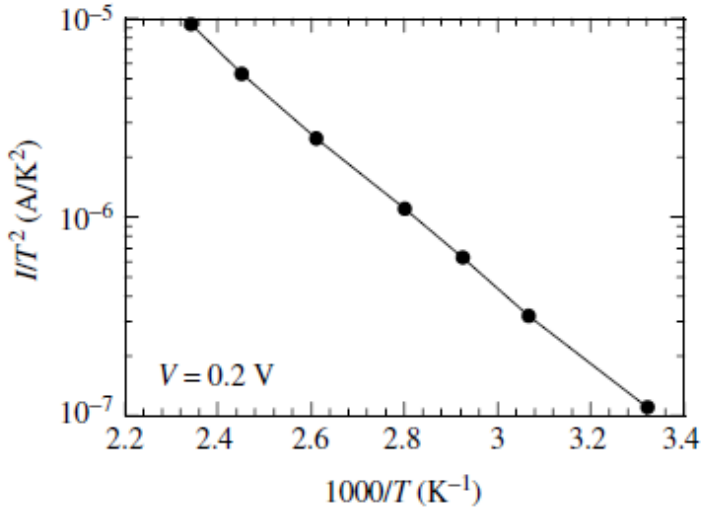

Fig. 3.39 Richardson plot of the "No Anneal" diode in Fig. 3.38 measured at $V = 0.2$ V.

3.5.3 $\emptyset_B$ from Capacitance-Voltage

- **Capacitance per unit area** of a Schottky diode

$$\frac{C}{A} = \sqrt{\frac{\pm q K_s \varepsilon_0 (N_A - N_D)}{2(\pm V_{bi} \pm V - kT/q)}} \qquad (3.50)$$

Reverse bias

+ for p-type ($N_A > N_D$)
- for n-type ($N_D > N_A$)

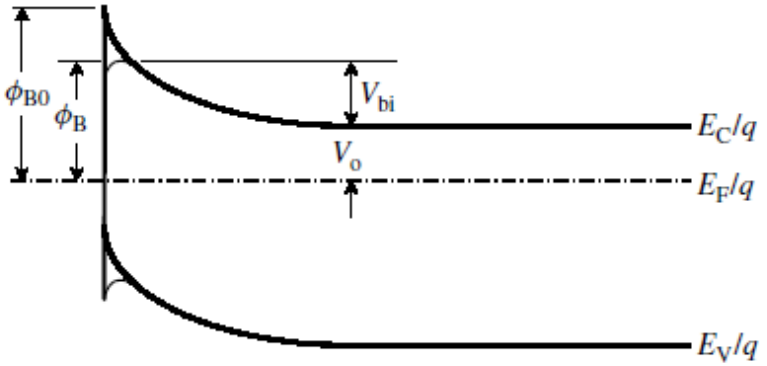

Fig. 3.36 Schottky barrier potential band diagram.

- From Fig.3.36, built-in potential (V_{bi}) related to barrier height ($\emptyset_B$)

$$\emptyset_B = V_{bi} + V_o \qquad (3.51)$$

- Barrier height $\emptyset_B$ is determined from the intercept voltage of Fig.3.40
  - almost flat band condition

$$\emptyset_B = -V_i + V_o + kT/q \qquad (3.52)$$

$V_o = (kT/q)\ln(N_C/N_D)$
Slope $2/[qK_s\varepsilon_0(N_A - N_D)]$

ϕ_B(C-V)=0.74 V

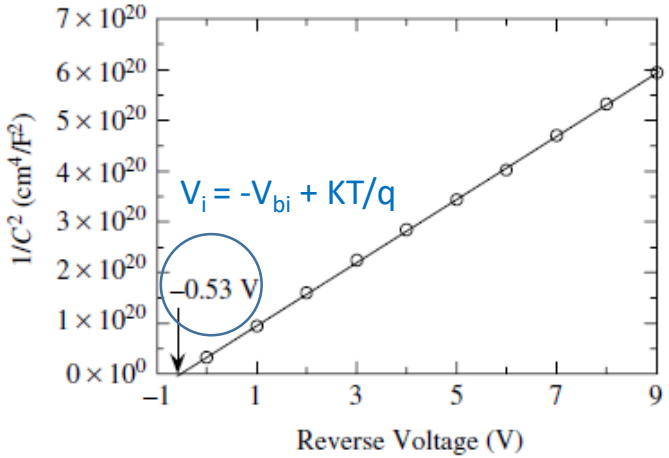

Fig. 3.40 Reverse-bias $1/C^2$ versus voltage of the "No Anneal" diode in Fig. 3.38 measured at room temperature.

H/W #2 (due to Oct 24th)

Chapter 3
(3.3)
(3.13)
(3.17)